COVID-19 induced lower-tropospheric ozone changes

Mertens, Mariano; Jöckel, Patrick; Matthes, Sigrun; Nützel, Matthias; Grewe, Volker; Sausen, Robert

DOI
10.1088/1748-9326/abf191

Publication date
2021

Document Version
Final published version

Published in
Environmental Research Letters

ENVIRONMENTAL RESEARCH
LETTERS

LETTER • **OPEN ACCESS**

COVID-19 induced lower-tropospheric ozone changes

ENVIRONMENTAL RESEARCH
LETTERS

LETTER

COVID-19 induced lower-tropospheric ozone changes

Mariano Mertens[1,*], Patrick Jöckel[1], Sigrun Matthes[1], Matthias Nützel[1], Volker Grewe[1,2] and Robert Sausen[1]

[1] Deutsches Zentrum für Luft- und Raumfahrt, Institut für Physik der Atmosphäre, Oberpfaffenhofen, Germany
[2] Delft University of Technology, Faculty of Aerospace Engineering, Section Aircraft Noise and Climate Effects, Delft, The Netherlands
[*] Author to whom any correspondence should be addressed.

E-mail: mariano.mertens@dlr.de

Keywords: COVID-19, air quality, ozone, source attribution

Supplementary material for this article is available online

OPEN ACCESS

RECEIVED
25 January 2021

REVISED
16 March 2021

ACCEPTED FOR PUBLICATION
24 March 2021

PUBLISHED
18 May 2021

Abstract

The recent COVID-19 pandemic with its countermeasures, e.g. lock-downs, resulted in decreases in emissions of various trace gases. Here we investigate the changes of ozone over Europe associated with these emission reductions using a coupled global/regional chemistry climate model. We conducted and analysed a business as usual and a sensitivity (COVID19) simulation. A source apportionment (tagging) technique allows us to make a sector-wise attribution of these changes, e.g. to natural and anthropogenic sectors such as land transport. Our simulation results show a decrease of ozone of 8% over Europe in May 2020 due to the emission reductions. The simulated reductions are in line with observed changes in ground-level ozone. The source apportionment results show that this decrease is mainly due to the decreased ozone precursors from anthropogenic origin. Further, our results show that the ozone reduction is much smaller than the reduction of the total NO_x emissions (around 20%), mainly caused by an increased ozone production efficiency. This means that more ozone is produced for each emitted NO_x molecule. Hence, more ozone is formed from natural emissions and the ozone productivities of the remaining anthropogenic emissions increase. Our results show that politically induced emissions reductions cannot be transferred directly to ozone reductions, which needs to be considered when designing mitigation strategies.

1. Introduction

The COVID-19 pandemic has a strong socio-economic impact [1]. As one consequence, in 2020 reduced carbon dioxide (CO_2) emissions from various sectors have been noted in many regions worldwide (e.g. [2, 3]). Typically, such reductions of CO_2 emissions are expected to be related to air quality improvements through reduced co-emission of pollutants. Indeed, reductions of particulate matter and nitrogen-dioxide (NO_2) have been observed in northern China [4]. In the case of NO_2 a reduction has also been observed from space in various regions all over the world [5]. However, it was also noted that ozone surface levels have partly increased despite the decrease of emissions of the ozone precursor NO_2 (e.g. [4, 6]).

This increase is due to the complex (nonlinear) ozone chemistry, which explains that a reduction in ozone precursors can lead to increasing ozone production, if the ozone production takes place in the 'VOC-limited' regime (e.g. [1, 6–9]). The emission reduction during spring 2020 related to COVID-19 is a rare real-life experiment from a scientific viewpoint [1], similar to the eruption of Eyjafjallajökull in 2010, which halted air-traffic for a short period in the affected regions (e.g. [10, 11]).

In this study we analyse the impact of strong emission reductions, observed during the first half of 2020, on the ozone chemistry by comparing the results of a business as usual (BAU) simulation and a simulation with strongly reduced emissions (COVID19). Additionally, we compare ground-level measurements during 2020 with measurements from previous years.

For our simulations we employ a regional chemistry climate model (CCM) on-line nested into a global CCM, which is relaxed to operational meteorological analysis, to assess the impact of reduced emissions on boundary layer ozone in Europe. To complement previous results based on observations, which are subject to changes in both, meteorology and emissions, and hence more difficult to interpret ([5, 6]) we use the CCM in a so-called quasi-chemistry transport model (QCTM) mode to suppress feedback from chemistry on meteorology [12]. Furthermore, our model setup allows for an attribution of ozone to various emission sectors (e.g. land transport, aviation, shipping) via a tagging technique as described by [13–15].

This paper is structured as follows: section 2 contains the description of the atmospheric model(s) and simulation set-ups along with the emission scenarios and a short description of the measurement data employed. The results are presented in section 3. Finally, we discuss our results (section 4) and state our conclusions (section 5).

2. Methods

2.1. Atmospheric modelling and simulation set-up

For our analyses we employ the CCM MECO(n) (MESSy-fied ECHAM COSMO models nested *n*-times) in a modified version of MESSy 2.54 ([16, 17]). Here, we use a MECO(1) setup which nests one instance of the regional CCM COSMO-CLM/MESSy [18] into the global CCM EMAC using the MESSy infrastructure ([19, 20]). COSMO–CLM is the community model of the German regional climate research community jointly further developed by the CLM-Community [21]. EMAC in turn uses the general circulation model ECHAM5 [22] as a base model. Our simulations cover the period 1 March–1 July 2020.

The global model, EMAC, was operated at a T42L90MA triangular spectral resolution, which corresponds to a quadratic Gaussian grid of approximately 2.8° × 2.8° (roughly 300 km) and 90 model levels in the vertical, which extend up to the middle atmosphere (∼0.01 hPa). Meteorological prognostic variables, i.e. divergence, vorticity, temperature (excluding mean temperature) and (logarithm of) surface pressure, have been 'nudged' by Newtonian relaxation to European Centre for Medium-Range Weather Forecasts (ECMWF's) operational analyses data for the simulation period with 6 h temporal resolution. The nudging coefficients are applied in a way that the large-scale synoptic patterns follow the ECMWF data, but the model can develop its own small-scale dynamics (for more details see [23]).

At the nesting boundaries, the global model passes boundary conditions with respect to dynamics and chemistry to the regional model with a high temporal resolution [17]. In this simulation, the regional COSMO refinement (nest) is centred over the North Atlantic and covers Europe, the North Atlantic and parts of North America with a resolution of approximately 50 km (see figure 1). The regional model is only forced by the boundary conditions and otherwise evolves freely.

Chemistry schemes for gas and aqueous phase chemistry are applied consistently in the global model and the regional refinement as described by [17]. For calculation of chemical kinetics, we use the MESSy submodel Module Efficiently Calculating the Chemistry of the Atmosphere (MECCA [24]). The chemical mechanism includes the chemistry of ozone, methane, and odd nitrogen. Alkynes and aromatics are not considered, but alkenes and alkanes are considered up to C_4. The Mainz Isoprene Mechanism (MIM1 [25]) is applied for the chemistry of isoprene and some non-methane hydrocarbons. Scavenging of trace gases by clouds and precipitation is calculated by the submodel SCAV (scavenging of traces gases by clouds and precipitation [26]). Dry deposition is considered according to [27].

To avoid feedbacks of the chemistry on dynamics, the global and the regional models are operated in the so-called QCTM mode [12]. In this mode mixing ratios of greenhouse gases with respect to the calculation of radiative fluxes are prescribed from daily averaged values of a previous simulation. This previous simulation covers the same time period and uses the same set-up as the BAU simulation described below. Due to the usage of the QCTM-mode the emission sensitivities described in section 2.2 do not affect the meteorological situation. This means, that in both simulations the meteorology (i.e. wind, temperature, humidity etc.) is identical. The transport and processing of chemical constituents is, however, different due to the changed primary emissions.

Anthropogenic and natural emissions are prescribed by flux conditions at the lower boundary. In our reference or BAU simulation anthropogenic emissions are prescribed according to the EDGAR 4.3.1 emission inventory for the year 2010 [28]. From the emission sectors in EDGAR 4.3.1 we distinguish the emission sectors land transport (TRA), anthropogenic non-traffic fossil fuel use in industry and households (in the following referred to ANT emissions, ANT), and shipping. Emissions of agricultural waste burning, biomass burning and aviation are prescribed according to the RCP 8.5 emission inventory for the year 2020 [29, 30].

Biogenic emissions of soil NO_x and biogenic isoprene are interactively calculated by the global and the regional model according to the parameterisations of [31] and [32], respectively. NO_x emissions from lightning are parameterised based on the cloud-top height [33] and scaled to global total emissions of ∼5 Tg(N)/a. The emissions of lightning-NO_x are

Table 1. Assumed emission reductions (in per cent) in the COVID19 sensitivity simulation compared to the BAU simulation. The total emissions are given in the supplement (section S3).

Sector/Region	Land transport (TRA)	Anthropogenic non-traffic (ANT)	Shipping (Ship)	Aviation (Avia.)
Europe (EU)	−50%	−30%		
East Asia (EA)	−20%	−30%		
North America (NA)	−20%	−30%		
Rest of the world (RoW)	−30%	−20%		
Globally			−20%	−90%

calculated in EMAC only and mapped to the finer resolved model instance (see [17]).

The source attributions method (tagging) is an accounting system following the relevant reaction pathways and is based on the method introduced by [34]. This diagnostic method allows to completely decompose the budgets of considered chemical species into contributions of sources. For the source attribution, the source terms, e.g. emissions, of the considered chemical species (odd oxygen, NO_y, CO, PAN, VOCs, OH and HO_2), are fully decomposed into N unique categories. In the present study we distinguish $N = 16$ different tagging categories (see section S4 in the supplement (available online at stacks.iop.org/ERL/16/064005/mmedia)). The details of the tagging method are described by [14] and [15] and the application in MECO(n) is demonstrated by [35]. The source attribution method allows us to separate the contributions of natural sources (tagging categories: stratosphere, CH_4, biogenic, N_2O, biomass burning and lightning) and anthropogenic emissions (all other sources, see section S4 in the supplement).

We have performed two simulations, which both use the same meteorology: BAU (BAU, with the reference emissions described above) and COVID19, which assumes emission reductions in the sectors land transport (TRA), ANT, shipping and aviation as described in section 2.2.

2.2. Assumptions on emissions during first half of 2020

For the COVID19 simulation we scale all emission sectors/species (CO, NO_x, SO_2, NH_3, and VOC) contained in the EDGAR 4.3.1 inventory and the aviation NO_x emissions of the RCP 8.5 emission inventory (table 1) in order to represent the reduced anthropogenic activities in individual regions of the globe. The reduction factors are constant over the whole simulation period (1 March–1 July 2020). Total emissions are given in the supplement (section S3).

BAU and COVID19 use the same initial conditions, but different emissions starting from 1 March 2020. Current estimates of rescaled emission factors for early to mid-2020 show large uncertainties and strong temporal variability (see figures 2–6 in [36]). Our study is highly idealized (e.g. by assuming time-independent reductions) and the assumed reductions should be seen as first-order estimates and were chosen during the early phase of the COVID-19 pandemic. Further, the qualitative conclusions (see next sections) are not critically dependent on the exact emission reductions.

A reduction of 30% has been assumed for ANT emissions (comprising industry and households) in Europe (EU), North America (NA) and East Asia (EA) and of 20% for the rest of the world (RoW). TRA emissions have been reduced by 30%, 20% and 20% in RoW, NA and EA, respectively, while a higher reduction factor of 50% has been assumed in EU. Our estimates of emissions in Europe are in line with emission reduction factors for individual countries in Europe estimated to be mostly in the order of 10%–30% for industry and 30%–80% for road transport [37]. Shipping emissions have been reduced by 20%, and aircraft emission by 90%, following ICAO movement data [38], which estimate a reduction of 94% in global aircraft movements.

2.3. Measurement data

As observational data (for the period 2017–2020) we used the air quality E1a & E2a data sets (formerly known as AirBase) available at [39]. We have set negative concentrations or unrealistic large concentrations to missing values for further analyses. In total this corresponds to less than 0.2% of all datapoints which are used in our analysis. As the resolution of our model does not account for localised effects [35], we use only data of stations which are classified as 'background'-stations (dataflag *AirQuality StationType*) in an area classified as either 'remote' or 'remote-rural' (dataflag *AirQualityStationArea*).

We chose the subset of stations (in total 273), which are available for the whole period for our analyses (section S7 in the supplement).

Similar to many comparable models (e.g. [40]), MECO(n) has deficits in simulating the night time ozone [35]. Usually, the simulated ozone levels during night are too high, while the model is able to capture the ozone peak during day. Therefore, the comparison of model results and measurements is restricted to the period 10–17 UTC.

To compare the model results with the measurements, we sample the one-hourly instantaneous model output at the lowest model layer at the

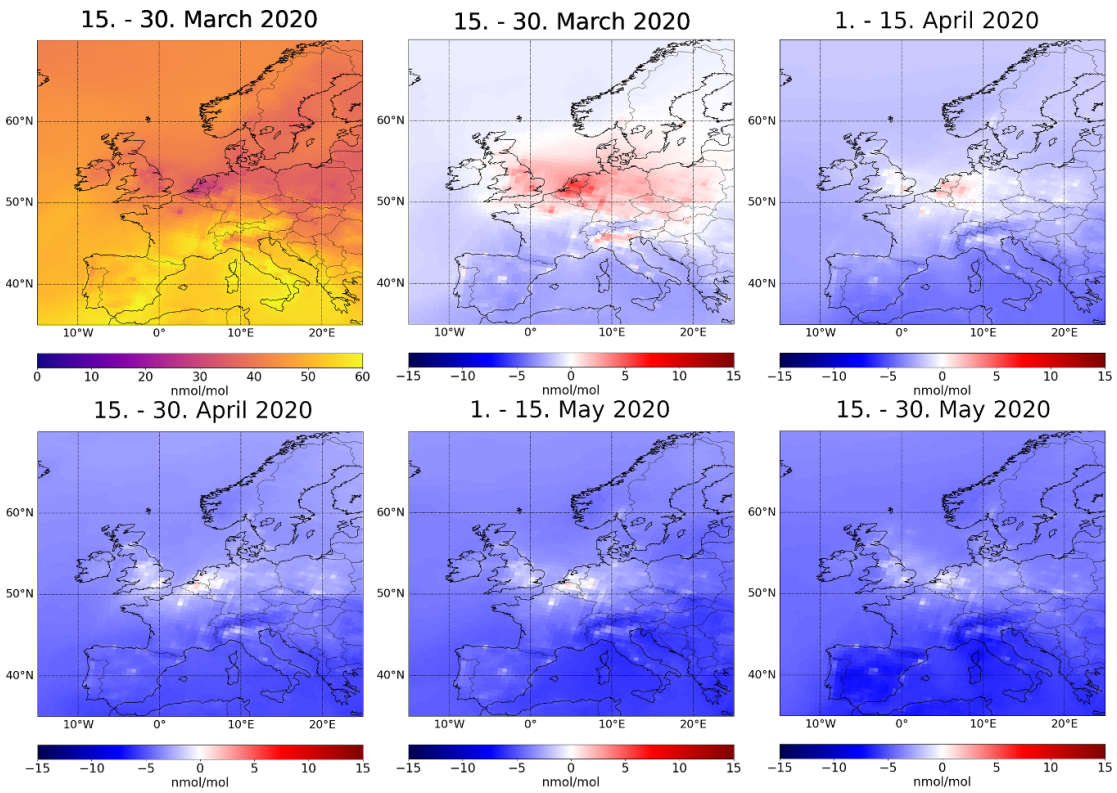

Figure 1. Ground-level ozone in nmol mol^{-1} over Europe for 15–30 March 2020 as simulated by BAU (upper left). Other panels show differences of (COVID19-BAU) of ground-level ozone (in nmol mol^{-1}) for the indicated periods.

positions of the respective observation stations. All datapoints, which are missing in the observational data for the year 2020, were set to missing values also for the model data.

3. Results

3.1. Lower tropospheric ozone response to emission reductions

In our analyses we focus on the results of the regional model over the area 15 °W–25 °E to 35 °N–70 °N (as shown in figure 1), which is centred over Europe. Hence, we will refer to quantities over this domain as European values. Further, we focus on the period March–May 2020.

The simulated near-surface ozone under BAU conditions shows large temporal variability over Europe during the analysed period (figure 2 and figure S1 in the supplement). The lower tropospheric ozone column (LTC; from the surface up to 850 hPa) increases from around 5 DU in March to up to ∼7 DU in May 2020 due to increased ozone production arising from increased photochemical activity in the course of the year. We choose 850 hPa as upper boundary of the LTC as this typically includes the planetary boundary layer everywhere in Europe except over the alpine region. The peaks with large values of the ozone column especially mid of April are mainly related to events in which high pressure ridges transport ozone rich air masses from lower latitudes to Europe. The reduction of anthropogenic emissions due to COVID-19 continuously reduces the ozone production, resulting in a by 0.6 DU smaller increase of LTC by the end of May. Due to the same dynamics of both simulations the part of the variability driven by meteorology is aligned.

The ozone production efficiency (OPE), i.e. the net-ozone production per NO_x molecule, however, increases in the COVID19 simulation compared to BAU (supplementary material figures S2 and S3 and section S2 for the definition). In addition, the commonly used indicator of the ozone production regime, the ratio of the production rate of H_2O_2 to the production rate of HNO_3 [41], also increases everywhere (figures S4 and S5 in the supplement). This indicates a shift of ozone production from a NO_x-saturated or intermediate to a NO_x-limited regime, in line with previous findings e.g. by [9].

As a consequence, the contribution of natural emission sources to the ozone LTC increases by 0.1–0.2 DU (figure 2 lower panel), despite unchanged emissions and partly counteracts the decrease of ozone of around 0.7 DU from anthropogenic sources (figure 2 bottom).

The change in OPE (cf. figures S2 and S3 in the supplement) is not uniform over Europe. Especially during 15–30 March an increase in ozone due to the COVID-19 related emission reduction is simulated in the area of the Benelux countries and only

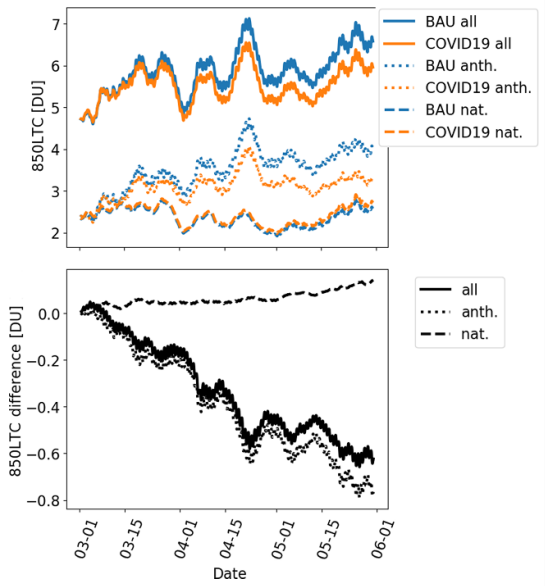

Figure 2. Lower tropospheric ozone columns in DU (for pressure higher than 850 hPa) averaged over the region shown in figure 1. (Top) Total lower tropospheric columns for the (blue) BAU and the (orange) COVID19 simulation for (solid) all, (dotted) anthropogenic and (dashed) natural sources. The latter two are diagnosed by the source apportionment method. (Bottom) Differences of the LTCs (COVID19-BAU) with line styles as in the top panel.

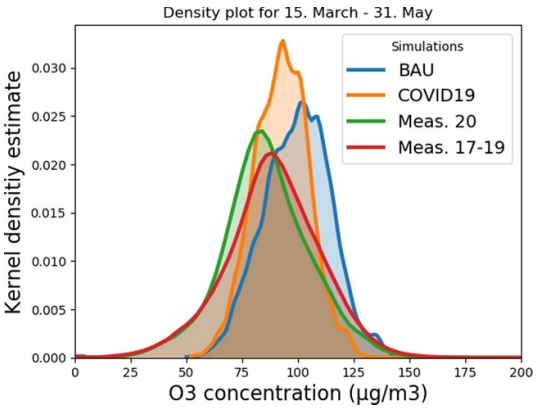

Figure 3. PDFs of ozone concentration at all 'rural'/'rural-remote' background stations for the BAU and COVID19 simulations as well as for the measurements of 2020 and the combinations of all measurements 2017–2019 (for the period 15 March–31 May).

after roughly a month this increased ozone vanishes and lower ozone mixing ratios compared to the BAU simulation dominate over Europe in the COVID19 simulation (figure 1). Large reductions of ozone are found in Southern Europe, except for the polluted metropolitan areas (e.g. around Madrid, Barcelona and Rome) and areas like the Po-valley. In these regions the OPE is rather low and favours an increase in ozone productivity with reduced emissions, counteracting the ozone production decrease from the reduction in precursor emissions. Averaged over the period 15 March–31 May the decrease of surface NO_x was between −10% and −40% over the different regions in Europe. At the same time, the reductions of ozone were only up to about −8% at maximum, while especially in Mid Europe ground-level ozone increased by up to 15% (see figure S6 in the supplement).

Our findings of lower ozone values in rural areas are largely supported by surface measurements (figure 3): The daytime measured ozone concentrations in rural areas have modal values of 89 and 84 μg m^{-3} in the pre-COVID-19 years (2017–2019) and during the COVID-19 pandemic (2020), respectively for spring (15 March–31 May), i.e. the probability density functions are shifted towards lower values (additional values are given in section S6 in the supplement). Here, we use the period 2017–2019 as an indicator of what might have happened without COVID-19, i.e. for comparison with the BAU simulation. Even though the model generally simulates larger mean ozone concentrations, the results show a shift of the modal values from 102 μg m^{-3} in BAU to 93 μg m^{-3} in COVID19. Hence, the shift towards lower values is similar to that of the measurements between 2017 to 2019 and 2020, but the magnitude is overestimated. Considering only ozone values around noon or around afternoon yields similar results (see figures S7 and S8 in the supplement). Also, the comparison of the difference between the daily ozone minimum and the daily ozone maximum showed similar biases (see figure S9 in the supplement). In general, however, the difference between the BAU and COVID19 simulation shows the same tendency as the difference between the measurements from 2020 and 2017–2019, respectively.

Of course, the difference between the measurements of 2017–2019 and 2020 is also influenced by the meteorological conditions, while the differences between our BAU and COVID19 simulations is caused by the emission reductions only. Nevertheless, the comparison of the measurement data indicates that a reduction of ground-level ozone due to the emission changes under COVID-19 conditions is very likely. This allows us to continue with our analysis of changes with respect to ozone sources related to the reduced emissions.

3.2. Attributing ozone reductions to emissions sectors

During May (1 May–30 May) the mean ozone LTC over the European domain (as depicted in figure 1) is roughly 6.1 and 5.6 DU for BAU and COVID19, respectively (see figure 2). The ozone decline in the COVID19 simulation stems from the reduction in anthropogenic emissions, which overcompensates the enhanced ozone productivity. This is caused by the reduction of ozone precursor emissions (mainly NO_x and VOCs) and the corresponding ozone increase related to natural sources,

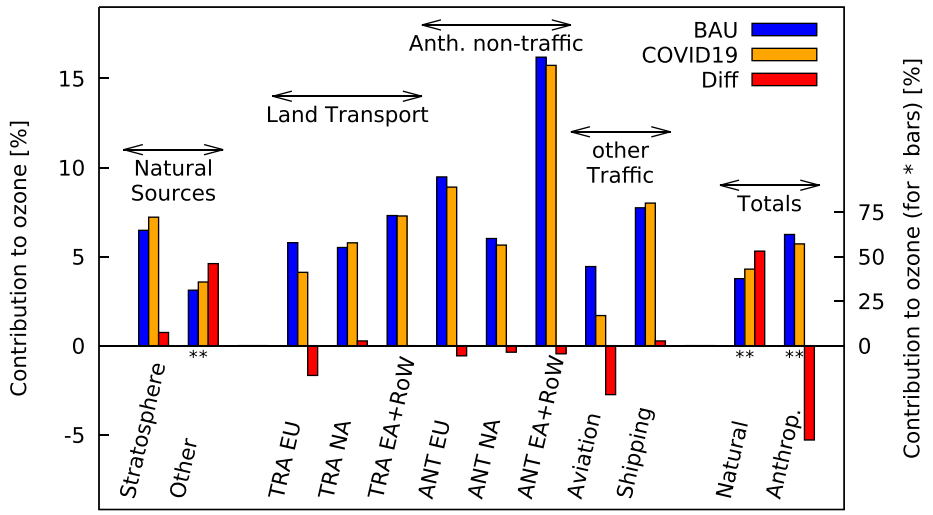

Figure 4. Contributions to lower tropospheric ozone columns (in percent) in the BAU (blue), COVID19 (orange) simulation and their differences (red, in percentage-points) during May 2020. Avia. is aviation and ship is shipping. Other natural sources include emissions from lightning, soils, biomass burning and methane depletion. Categories marked with two asterisks refer to the vertical axis on the right, all others to the vertical axis on the left.

such as soil emissions, biomass burning, lightning and methane depletion (figure 4). The absolute value of mean LTC from natural (anthropogenic) sources increases (decreases) from approximately 2.3 (3.8) DU to roughly 2.4 (3.2) DU from BAU to COVID19. This translates to relative contributions of natural emissions to the mean LTC over Europe of roughly 37% and 43% in BAU and COVID19, respectively.

The relative contributions of almost all anthropogenic emissions sectors to the LTC decrease (figure 4). The sectors with the largest contribution decrease to LTC ozone are the aviation sector (90% emission reduction) with a decrease of 2.7% points and the TRA sector in Europe (50% emission reduction) with a decrease of 1.6% points. This corresponds to an overall decrease of the contribution of anthropogenic emissions from roughly 63% to 57%. The relative contribution of the emission sectors TRA NA and shipping increase slightly, but their absolute contributions (section S5 in the supplement) decrease indicating that the ozone productivity of these two sectors increases slightly more than in the other emission sectors and regions.

Further, our results indicate that European emissions (i.e. TRA EU + ANT EU) contribute only around 15% (BAU) and 13% (COVID19) to lower tropospheric ozone in Europe during May 2020. All other anthropogenic emissions (i.e. shipping, aviation, non-EU TRA and non-EU ANT) contribute roughly 48% (BAU) and 44% (COVID19). This clearly indicates the well-known importance of long-range transport for ozone pollution (e.g. [42]). In addition, the change of the chemical regime implies an increase of the ozone lifetime, since a reduction of ozone leads to a reduction of OH and therefore HO_x related ozone depletion rates in the troposphere (e.g. [43, 44]). This can be seen by the increased contribution of stratospheric ozone to the LTC of ozone from 6.5% to 7.3% (figure 4). As stratospheric ozone is unperturbed in our COVID19 simulation the influx to the troposphere is almost unchanged. Therefore, the increase of the contribution of ozone from the stratosphere indicates an increase of the tropospheric ozone lifetime. The absolute contribution of stratospheric ozone to the LTC increases by around 2%, indicating an increase of the ozone lifetime of 2%.

4. Discussion

By design our study is highly idealized as we assume that the emission reductions take place world-wide at the same time and without temporal variability from March to June. There are first studies, which present more detailed emission modelling for Europe and Asia (e.g. [36, 37, 45, 46]). Generally, our assumed reductions are in line with [36] however our estimates for EA ANT and shipping are slightly larger, whereas NA TRA reductions are somewhat low. However, the estimates presented in [36] show considerable uncertainties. Our results need to be interpreted while keeping these simplifications in mind.

Compared to, e.g. [45, 47], our study analyses for the first time the impact of the emission reduction on ozone using a source apportionment method. This method allows a more detailed understanding of the changes of the ozone chemistry and is able to attribute the changes to certain emission sectors. Therefore, our study delivers important additional insights.

Even though our emission reductions in Europe of −50% and −30% of LT and ANT, respectively, are very large, we see only a rather small decrease of mean lower tropospheric ozone columns

of around 8% during May 2020 over Europe (see figure 2). The main reason for this is the increasing OPE per NO_x molecule (see definition of the OPE in the supplement). This leads to a small increase (∼0.1 DU) in the ozone values produced from natural emissions (figures 2 and 3). With respect to potential mitigation options this result demonstrates that detailed assessments are needed to judge, whether planned emissions reductions are sufficient to decrease tropospheric ozone burdens substantially. Indeed, some modelling studies (e.g. [45, 47]) indicate a similarly low response of ozone. Some measurement studies (e.g. [4, 6, 48–50]) even found an increase of ozone near city centres during March 2020 compared to previous years, probably due to decreased NO_x emissions. However, also the role of meteorology needs to be considered [51].

Our study further highlights that due to the rather long lifetime of ozone, the emissions in other parts of the world strongly influence European ozone levels. Therefore, reducing emissions only in Europe will most likely not lead to envisaged ozone decreases in Europe.

Our simulation results show that around three months are needed until the difference of the ozone LTC between BAU and COVID19 (see figures 2 and S1) equilibrates. In most countries the strong emission reductions took place for some weeks, only (e.g. [37]). Therefore, the actual effect of the emission reductions during COVID-19 in spring 2020 is likely to be much smaller than the maximum signal of our idealized study.

Due to the uncertainty of the applied emission inventory for BAU and the non-linearity of the ozone production (e.g. 13) our simulated response of the emission reduction (figure 2) might still be overestimated, if our BAU emissions are underestimated. Indeed, the shift of ozone values between our BAU and COVID19 simulation is larger as the shift in the measurements from 2017 to 2019 and 2020. This could indicate an overestimated response, but this difference could also be caused by differences of the meteorological conditions in the previous years (2017–2019) compared to 2020.

The main focus of our study is on near ground-level ozone, focusing mainly on-air quality related issues. Besides this, changes in ozone and other emissions influence also the climate. However, as already been shown by [3], the overall climate impact of the strong emission reductions during COVID-19 is small. According to [3], the decrease of ozone precursors leads to a short-term cooling, which is offset by a warming effect due to less aerosol.

5. Conclusion

We conducted a sensitivity experiment (COVID19) to analyse the processes occurring with respect to lower tropospheric ozone in a period of reduced anthropogenic emissions as during the recent COVID-19 pandemic compared to an emission scenario without the impact of the COVID-19 pandemic (BAU). Our simulations with a coupled global and regional CCM and a source attribution technique show:

- the ozone LTC averaged over the European domain in the COVID19 simulation become continuously lower over time for around three months compared to the BAU simulation before a new equilibrium is reached.
- there are large spatial inhomogeneities with respect to this overall trend in ozone LTCs, which are related to the ozone production regimes.
- the overall shift towards smaller ozone LTCs in COVID19 and BAU is also found in measurement data from ground-based stations.
- changes in anthropogenic emissions cause the changes in ozone LTCs and are to some degree compensated by enhanced ozone productivity from natural sources. Due to the increase of the OPE the reductions in ozone are much smaller than the emission reductions. In our case NO_x at ground-level is reduced by up to 40% in Europe, while ground-level ozone changes are in the range of −8% to +15% for Europe.

The results of our study are not only relevant for ozone changes related to the recent reduction in emissions due to the COVID19 pandemic, they also are a starting point for discussing mitigation strategies. In line with our model results, measurements during the first half of 2020 and first modelling studies show ozone responses which are much smaller than the emission reductions. This indicates that strong emission reductions are needed world-wide to achieve substantially reduced tropospheric ozone levels.

Data availability statement

The data that support the findings of this study are available upon reasonable request from the authors.

Acknowledgments

We thank Astrid Kerkweg, FZ Jülich, for her ongoing support and the MECO(n) developments and Christoph Kiemle, DLR, for very helpful comments improving the quality of the manuscript. Further, we thank the MESSy consortium and the CLM-Community for their model developments and ongoing support. The work described in this paper received funding from the DLR projects TraK (Transport und Klima) and Eco2Fly and by the Initiative and Networking Fund of the Helmholtz Association through the project 'Advanced

Earth System Modelling Capacity' (ESM). Individual authors receive funding from the European Union's Horizon 2020 research and innovation programme under Grant Agreement No. 875036 within the Aeronautics project ACACIA. We thank the ECWMF for providing operational meteorological analysis. This work used resources of the Deutsches Klimarechenzentrum (DKRZ) granted by its Scientific Steering Committee (WLA) under project ID bd0617.

ORCID iDs

Mariano Mertens https://orcid.org/0000-0003-3549-6889
Patrick Jöckel https://orcid.org/0000-0002-8964-1394
Sigrun Matthes https://orcid.org/0000-0002-5114-2418
Volker Grewe https://orcid.org/0000-0002-8012-6783
Robert Sausen https://orcid.org/0000-0002-9572-2393

References

[1] Diffenbaugh N S *et al* 2020 The COVID-19 lockdowns: a window into the earth system *Nat. Rev. Earth Environ.* **1** 470–81
[2] Le Quéré C *et al* 2020 Temporary reduction in daily global CO_2 emissions during the COVID-19 forced confinement *Nat. Clim. Change* **10** 647–53
[3] Forster P M *et al* 2020 Current and future global climate impacts resulting from COVID-19 *Nat. Clim. Change* **10** 913–9
[4] Shi X and Brasseur G P 2020 The response in air quality to the reduction of Chinese economic activities during the COVID-19 outbreak *Geophys. Res. Lett.* **47** e2020GL088070
[5] Bauwens M *et al* 2020 Impact of coronavirus outbreak on NO_2 pollution assessed using TROPOMI and OMI observations *Geophys. Res. Lett.* **47** e2020GL087978
[6] Keller C A *et al* 2021 Global impact of COVID-19 restrictions on the surface concentrations of nitrogen dioxide and ozone *Atmos. Chem. Phys.* **21** 3555–92
[7] Dodge M 1977 Combined use of modeling techniques and smog chamber data to derive ozone precursor relationships *Int. Conf. on Photochemical Oxidant Pollution and Its Control: Proc.* vol II, ed B Dimitriades (Research Triangle Park, NC: U.S. Environmental Protection Agency, Environmental Sciences Research Laboratory) pp 881–9 EPA/600/3-77-001b
[8] Lin X, Trainer M and Liu S C 1988 On the nonlinearity of the tropospheric ozone production *J. Geophys. Res.* **93** 15879–88
[9] Grewe V, Dahlmann K, Matthes S and Steinbrecht W 2012 Attributing ozone to NOx emissions: implications for climate mitigation measures *Atmos. Environ.* **59** 102–7
[10] Gislason S R *et al* 2011 Characterization of Eyjafjallajökull volcanic ash particles and a protocol for rapid risk assessment *Proc. Natl Acad. Sci.* **108** 7307–12
[11] Turnbull K, Johnson B, Marenco F, Haywood J, Minikin A, Weinzierl B, Schlager H, Schumann U, Leadbetter S and Woolley A 2012 A case study of observations of volcanic ash from the Eyjafjallajökull eruption: 1. *In situ* airborne observations *J. Geophys. Res.* **117** D00U12
[12] Deckert R, Jöckel P, Grewe V, Gottschaldt K-D and Hoor P 2011 A quasi chemistry-transport model mode for EMAC *Geosci. Model Dev.* **4** 195–206
[13] Grewe V, Tsati E and Hoor P 2010 On the attribution of contributions of atmospheric trace gases to emissions in atmospheric model applications *Geosci. Model Dev.* **3** 487–99
[14] Grewe V, Tsati E, Mertens M, Frömming C and Jöckel P 2017 Contribution of emissions to concentrations: the TAGGING 1.0 submodel based on the modular earth submodel system (MESSy 2.52) *Geosci. Model Dev.* **10** 2615–33
[15] Rieger V S, Mertens M and Grewe V 2018 An advanced method of contributing emissions to short-lived chemical species (OH and HO2): the TAGGING 1.1 submodel based on the modular earth submodel system (MESSy 2.53) *Geosci. Model Dev.* **11** 2049–66
[16] Kerkweg A and Jöckel P 2012 The 1-way on-line coupled atmospheric chemistry model system MECO(n)—part 1: description of the limited-area atmospheric chemistry model COSMO/MESSy *Geosci. Model Dev.* **5** 87–110
[17] Mertens M, Kerkweg A, Jöckel P, Tost H and Hofmann C 2016 The 1-way on-line coupled model system MECO(n)—part 4: chemical evaluation (based on MESSy v2.52) *Geosci. Model Dev.* **9** 3545–67
[18] Kerkweg A and Jöckel P 2012 The 1-way on-line coupled atmospheric chemistry model system MECO(n)—part 2: on-line coupling with the multi-model-driver, (MMD) *Geosci. Model Dev.* **5** 111–28
[19] Jöckel P, Kerkweg A, Pozzer A, Sander R, Tost H, Riede H, Baumgaertner A, Gromov S and Kern B 2010 Development cycle 2 of the modular earth submodel system (MESSy2) *Geosci. Model Dev.* **3** 717–52
[20] Jöckel P *et al* 2016 Earth system chemistry integrated modelling (ESCiMo) with the modular earth submodel system (MESSy) version 2.51 *Geosci. Model Dev.* **9** 1153–200
[21] Rockel B, Will A and Hense A 2008 The regional climate model COSMO-CLM (CCLM) *Meteorol. Z.* **17** 347–8
[22] Roeckner E, Brokopf R, Esch M, Giorgetta M, Hagemann S, Kornblueh L, Manzini E, Schlese U and Schulzweida U 2006 Sensitivity of simulated climate to horizontal and vertical resolution in the ECHAM5 atmosphere model *J. Clim.* **19** 3771–91
[23] Jöckel P *et al* 2006 The atmospheric chemistry general circulation model ECHAM5/MESSy1: consistent simulation of ozone from the surface to the mesosphere *Atmos. Chem. Phys.* **6** 5067–104
[24] Sander R *et al* 2019 The community atmospheric chemistry box model CAABA/MECCA-4.0 *Geosci. Model Dev.* **12** 1365–85
[25] Pöschl U, Von Kuhlmann R, Poisson N and Crutzen P 2000 Development and intercomparison of condensed isoprene oxidation mechanisms for global atmospheric modeling *J. Atmos. Chem.* **37** 29–52
[26] Tost H, Jöckel P, Kerkweg A, Sander R and Lelieveld J 2006 Technical note: a new comprehensive SCAVenging submodel for global atmospheric chemistry modelling *Atmos. Chem. Phys.* **6** 565–74
[27] Kerkweg A, Buchholz J, Ganzeveld L, Pozzer A, Tost H and Jöckel P 2006 Technical note: an implementation of the dry removal processes DRY DEPosition and SEDImentation in the modular earth submodel system (MESSy) *Atmos. Chem. Phys.* **6** 4617–32
[28] Crippa M, Janssens-Maenhout G, Dentener F, Guizzardi D, Sindelarova K, Muntean M, Van Dingenen R and Granier C 2016 Forty years of improvements in European air quality: regional policy-industry interactions with global impacts *Atmos. Chem. Phys.* **16** 3825–41
[29] van Vuuren D P *et al* 2011 The representative concentration pathways: an overview *Clim. Change* **109** 5–31
[30] Riahi K, Rao S, Krey V, Cho C, Chirkov V, Fischer G, Kindermann G, Nakicenovic N and Rafaj P 2011 RCP 8.5—a scenario of comparatively high greenhouse gas emissions *Clim. Change* **109** 33–57
[31] Yienger J J and Levy H 1995 Empirical model of global soil-biogenic NO_x emissions *J. Geophys. Res. Atmos.* **100** 11447– 64

[32] Guenther A et al 1995 A global model of natural volatile organic compound emissions J. Geophys. Res. 100 8873–92
[33] Price C, Rind D 1992 A simple lightning parameterization for calculating global lightning distributions J. Geophys. Res. 97 9919–33
[34] Grewe V 2013 A generalized tagging method Geosci. Model Dev. 6 247–53
[35] Mertens M, Kerkweg A, Grewe V, Jöckel P and Sausen R 2020 Are contributions of emissions to ozone a matter of scale?—a study using MECO(n) (MESSy v2.50) Geosci. Model Dev. 13 363–83
[36] Doumbia T et al 2021 Changes in global air pollutant emissions during the COVID-19 pandemic: a dataset for atmospheric chemistry modeling Earth Syst. Sci. Data Discuss. (https://doi.org/10.5194/essd-2020-348)
[37] Guevara M et al 2021 Time-resolved emission reductions for atmospheric chemistry modelling in Europe during the COVID-19 lockdowns Atmos. Chem. Phys. 21 773–97
[38] ICAO (International Civil Aviation Organisation) 2020 Effects of novel coronavirus (COVID-19) on civil aviation: economic impact analysis ICAO 8 May 2020 (Montréal: Air Transportation bureau)
[39] European Air Quality Portal E1a & E2a data sets (available at: https://discomap.eea.europa.eu/map/fme/AirQualityExport.htm) (Accessed 8 January 2021)
[40] Travis K R and Jacob D J 2019 Systematic bias in evaluating chemical transport models with maximum daily 8 h average (MDA8) surface ozone for air quality applications: a case study with GEOS-Chem v9.02 Geosci. Model Dev. 12 3641–8
[41] Sillman S 1995 The use of NO_y, H_2O_2, and HNO_3 as indicators for ozone-NO_x-hydrocarbon sensitivity in urban locations J. Geophys. Res. 100 14175–88
[42] Monks P S et al 2015 Tropospheric ozone and its precursors from the urban to the global scale from air quality to short-lived climate forcer Atmos. Chem. Phys. 15 8889–973
[43] Stevenson D S et al 2006 Multimodel ensemble simulations of present-day and near-future tropospheric ozone J. Geophys. Res. 111 D08301
[44] Grewe V 2007 Impact of climate variability on tropos pheric ozone Science of The Total Environment. 374 167–81
[45] Menut L, Bessagnet B, Siour G, Mailler S, Pennel R and Cholakian A 2020 Impact of lockdown measures to combat Covid-19 on air quality over Western Europe Sci. Total Environ. 741 140426
[46] Xing J, Li S, Jiang Y, Wang S, Ding D, Dong Z, Zhu Y and Hao J 2020 Quantifying the emission changes and associated air quality impacts during the COVID-19 pandemic on the North China Plain: a response modeling study Atmos. Chem. Phys. 20 14347–59
[47] Dentener F, Emberson L, Galmarini S, Cappelli G, Irimescu A, Mihailescu D, Van Dingenen R and Van Den Berg M 2020 Lower air pollution during COVID-19 lock-down: improving models and methods estimating ozone impacts on crops Phil. Trans. R. Soc. A 378 20200188
[48] Lee J D, Drysdale W S, Finch D P, Wilde S E and Palmer P I 2020 UK surface NO2 levels dropped by 42 % during the COVID-19 lockdown: impact on surface O3 Atmos. Chem. Phys. 20 15743–59
[49] Sicard P, De Marco A, Agathokleous E, Feng Z, Xu X, Paoletti E, Rodriguez J J D and Calatayud V 2020 Amplified ozone pollution in cities during the COVID-19 lockdown Sci. Total Environ. 735 139542
[50] Salma I, Vörösmarty M, Gyöngyösi A Z, Thén W and Weidinger T 2020 What can we learn about urban air quality with regard to the first outbreak of the COVID-19 pandemic? A case study from central Europe Atmos. Chem. Phys. 20 15725–42
[51] Petetin H, Bowdalo D, Soret A, Guevara M, Jorba O, Serradell K and Pérez García-Pando C 2020 Meteorology-normalized impact of the COVID-19 lockdown upon NO_2 pollution in Spain Atmos. Chem. Phys. 20 11119–41